Proceedings of 14th IOE Graduate Conference
Peer Reviewed
Year: 2023 Month: December Volume: 14
ISSN: 2350-8914 (Online), 2350-8906 (Print)

Power System Voltage Stability Evaluation Considering Renewable Energy with Correlated Variabilities

Abanish Tiwari [a], Sandeep Dhami [b], Milan Subedi [c]

[a, b] *Department of Electrical Engineering, Pashchimanchal Campus, IOE, Tribhuvan University, Nepal*
[c] *Nepal Electricity Authority*
[a] abanish.782540@pasc.tu.edu.np, [b] sandeep.dhami@ioepas.edu.np, [c] ms@nea.org.np

Abstract
The world's energy outlook is shifting markedly towards sustainability and eco-friendliness. This entails integrating renewable sources like solar and wind power into conventional grids, bringing advantages like lower emissions and reduced fossil fuel dependency. Unlike stable fossil fuel plants, renewable generation varies due to weather-driven intermittency, affecting the voltage stability and loading capacity of the grid. This study focuses on evaluating the GSA and load margin of the system, employing the IEEE 9-bus system and the INPS of Lumbini Province. Results reveal a 1.46% system power loss, concentrated at Bus 5 due to minimal voltage levels. The study employs optimal power flow equations to assess load margins, with the most probable margin emerging at approximately 1.25 times the existing load for the analysis of Lumbini Province. Sensitivity analysis identifies key substations, with Butwal Grid SS deemed most influential. In Lumbini province, wind generation exhibits distinct characteristics across locations, while load flow analysis indicates varying voltage levels in substations. Correlation analysis highlights strong positive correlations among solar projects and low correlations with wind generation, emphasizing coordination opportunities. High load margin values affirm reliable power supply and sensitivity analysis underscores the crucial role of specific substations in power distribution. The PV and QV curves reveal potential voltage level drops with increased active and reactive loads and improvement in the voltage profile with the penetrations of RES.

Keywords
Correlated Variabilities, Renewable Energy, Sensitivity Analysis, Voltage Stability

1. Introduction

The global energy landscape is undergoing a significant transformation towards a more sustainable and environmentally friendly future. This transformation involves incorporating renewable energy sources, such as solar and wind power, into traditional power systems. These sustainable sources provide various advantages, such as a decrease in greenhouse gas emissions and reduced dependence on fossil fuels.

Renewable energy generation differs from conventional fossil energy generation in that it is very random and intermittent, having a substantial impact on branch currents, bus voltages, and grid losses. Unlike conventional power plants, which can provide a steady output, renewable energy generation is highly dependent on factors like weather conditions and sunlight availability. As a result, the power system's scheduling and control have grown increasingly challenging and intricate [1]. The growing adoption of renewable energy generation is now making its way into the power grid, leading to a notable rise in the unpredictability of the power system.

Hence, when integrating extensive renewable energy sources into the grid, it becomes imperative to conduct uncertainty assessments on the power system for monitoring and averting voltage collapse. In order to guarantee the dependable and effective operation of modern power systems, power system voltage stability is a critical factor. Power system voltage stability evaluation has become more difficult and complicated as Renewable Energy Sources (RESs) like wind and solar power are being integrated more and more into power grids. This is because RESs show correlated variabilities and are highly reliant on environmental variables, both of which have a big impact on the stability of the voltage in the power system. The voltage stability problem in power systems can result in voltage collapse, system instability, and eventually blackouts. Determining the voltage stability of power systems under various working scenarios, including the integration of RESs with correlated variabilities, is therefore crucial.

In recent years, several investigations have been carried out on stochastic power system challenges, including studies related to probabilistic load flow and small signal stability [2, 3, 4, 5, 6, 7]. Given the nature of variables, stochastic approaches have been developed to assess the erratic performance of power systems because conventional deterministic methods are unable to accurately capture their unique characteristics. The sensitivity of load margins with regard to several arbitrary parameters was calculated in [8, 9]. In paper [10], a global sensitivity analysis (GSA) method is suggested to rank the importance of renewable energy variables that will have an impact on the voltage stability of power networks with the determination of load margin.

In this paper, an efficient global sensitivity analysis (GSA) technique is suggested to evaluate the priority of renewable energy variables that will have an impact on the voltage stability of power systems. For this first, a probabilistic model for calculating the load margin while taking into account renewable energy generation will be presented. The sensitivity

index was derived for assessing the effects of such variables, and GSA was then applied to models with linked random input variables. The research will model the probability density function of the renewable energy sources i.e. PV and wind and also the load for the IEEE-9 bus system. The proposed method will then be tested using the IEEE 9-bus systems in this study.

2. Material and Methods

The various methods applied in the course of study are discussed in this section.

2.1 Obtain probability models of random input variables

The fluctuations in the direction of active load growth follow a normal distribution, with the associated probability distribution function (PDF) depicted in Eq. 1 [10].

$$f(b_{Pi}) = \frac{1}{\sqrt{2\pi\sigma_{bPi}^2}} \exp\left(-\frac{(b_{pi}-\mu_{bPi})^2}{2\sigma_{bPi}^2}\right) \quad (1)$$

The reactive power of the load can be similarly characterized to maintain a consistent power factor.

$$b_{Qi} = b_{Pi}\tan\alpha_L \quad (2)$$

In wind power generation, the Weibull model is frequently employed to depict wind speed, as indicated in the PDF outlined in [11].

$$f(v) = \left(\frac{k}{c}\right)\left(\frac{x}{c}\right)^{k-1}\exp\left(-\left(\frac{x}{c}\right)^k\right), v \geq 0 \quad (3)$$

Where, k, c: Parameters of a Weibull distribution; x: Input random variable vector

The output power p_w of WT is affected by wind speed as follows [4]:

$$p_w(v) = \begin{cases} 0 & v \leq v_{ci} \\ P_r\frac{v-v_{ci}}{v_r-v_{ci}} & v_{ci} \leq v \leq v_r \\ P_r & v_r \leq v \leq v_{co} \\ 0 & v > v_{co} \end{cases} \quad (4)$$

Wind power generators are typically linked directly to the electrical grid. A wind turbine (WT) operating at a constant power factor can be simplified as a PQ bus within the grid. The reactive power, denoted as q_w, for the WT can be expressed as follows:

$$q_w = p_w\tan\alpha_w \quad (5)$$

Photovoltaic (PV) electricity production relies on solar irradiance r, which is characterized by a Beta distribution.

$$f(r) = \frac{\Gamma(a+b)}{\Gamma(a)+\Gamma(b)}\left(\frac{r}{r_{\max}}\right)^{a-1}\left(1-\frac{r}{r_{\max}}\right)^{b-1} \quad (6)$$

Where, a, b: Parameters of a Beta distribution.

The active power generated by the photovoltaic system, Ps, is contingent upon solar irradiance and can be represented as follows:

$$P_s = rA\eta \quad (7)$$

Where, r = solar irradiance (W/m2); A=light-receiving area (m2); η= photoelectric conversion efficiency (%)

2.2 Determination of Load Margin

2.2.1 Objective Function:

The optimization model is given as follows [10]:

$$Max: \lambda \quad (8)$$

$$V_i\sum V_j\left|Y_{ij}\right|\cos\left(\theta_{ij}-\delta_{ij}\right)-(P_{Gi}+P_{Ri}-P_{Di}-\lambda b_{Pi}) = 0 \quad (9)$$

$$V_i\sum V_j\left|Y_{ij}\right|\sin\left(\theta_{ij}-\delta_{ij}\right)-\left(Q_{Gi}+Q_{Ri}-Q_{Di}-\lambda b_{Qi}\right) = 0 \quad (10)$$

$$P_{Gi,\min} \leq P_{Gi} \leq P_{Gi,\max} \quad (11)$$

$$Q_{Gi,\min} \leq Q_{Gi} \leq Q_{Gi,\max} \quad (12)$$

$$V_{i,\min} \leq V_i \leq V_{i,\max} \quad (13)$$

$$P_{Lij} = -t_{ij}G_{ij}V_i^2 + V_iV_j\left(G_{ij}\cos\theta_{ij}+B_{ij}\sin\theta_{ij}\right) \quad (14)$$

$$Q_{Lij} = t_{ij}B_{ij}V_i^2 - B_{ij}V_i^2/2 + V_iV_j\left(G_{ij}\sin\theta_{ij}+B_{ij}\cos\theta_{ij}\right) \quad (15)$$

$$P_{Lij}^2 + Q_{Lij}^2 \leq S_{Lij,\max}^2 \quad (16)$$

2.3 Generation of Correlated Samples

The Nataf inverse transformation approach is used to acquire samples of power generation from renewable sources that exhibit correlation. This methodology is depicted in Figure 1.

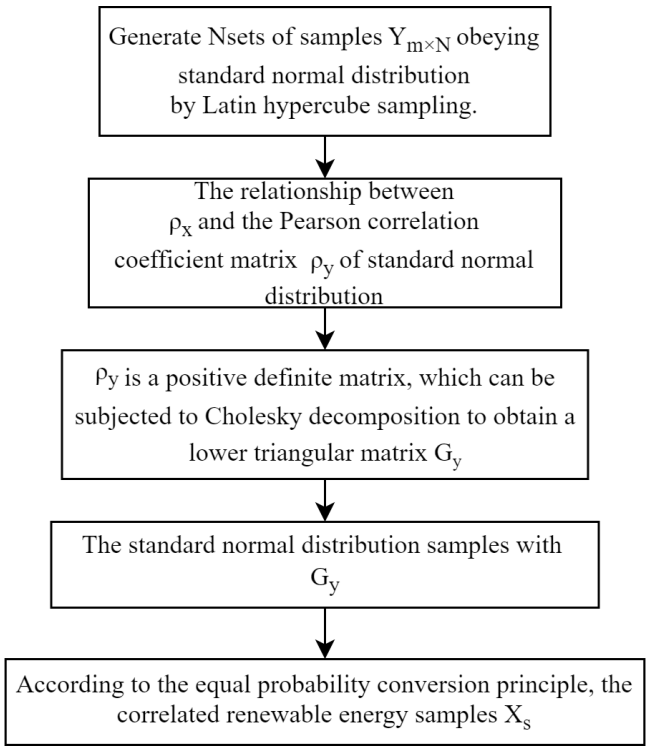

Figure 1: Flowchart for generating samples of correlated variables.

2.4 Evaluation of the GSA indices

The calculation process is illustrated in Figure 2.

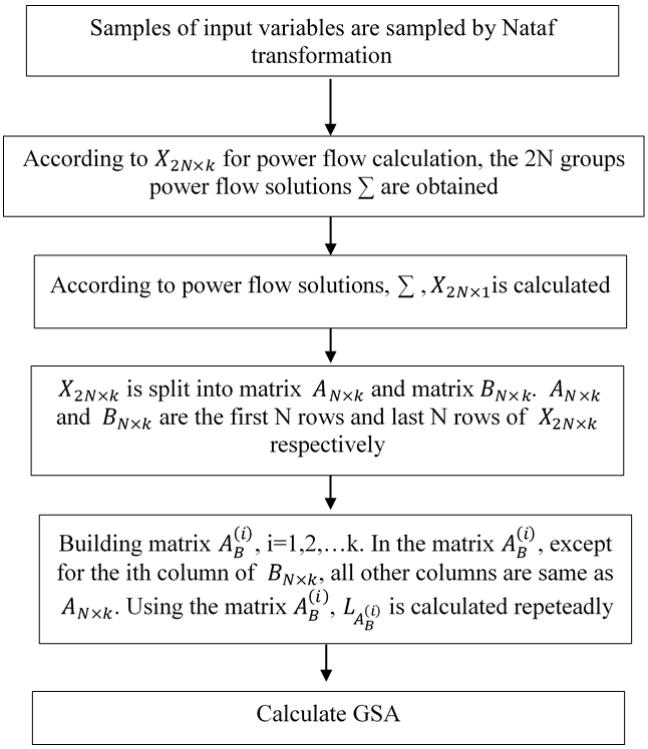

Figure 2: Calculation of the GSA

2.5 Tools

Python programming language is used for the overall process of determination of correlated variables and load margin.

3. Result and Discussion

With the aforementioned methodology, the analysis for the IEEE-9 bus system and the INPS for Lumbini Province was carried out the results obtained during the process are described herewith.

3.1 IEEE-9 bus system

The results obtained from the analysis of IEEE-9 bus system is described in this section.

3.1.1 Wind Model

The probability distribution curve for the wind velocity is derived with the Weibull model is shown in Figure 3. The values of k and c are considered to be 2.06 and 7.41 respectively [10]. The results indicate that the highest probability of the occurrence of wind is with a velocity of around 6 m/s. Also, there is a very low probability of the occurrence of a velocity higher than 20 m/s. This information is crucial for designing wind turbines and assessing the potential energy production from a wind farm.

3.1.2 PV Model

Also, the sample of level of solar irradiance is obtained from the beta distribution as in the Figure 4. The parameters a and b

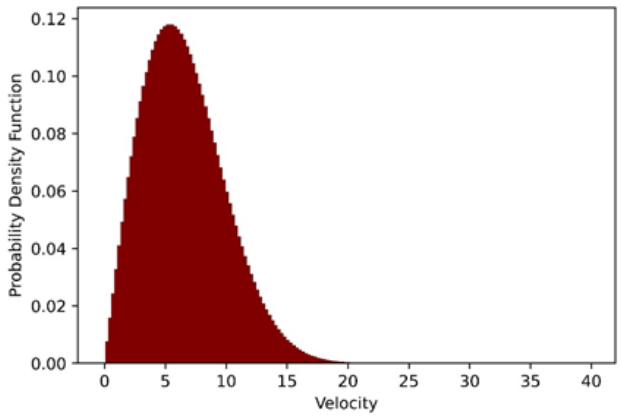

Figure 3: PDF of wind velocity using Weibull model

are considered to be 2.06 and 2.5 respectively. The probability of occurrence of irradiance 0.4 has the highest probability.

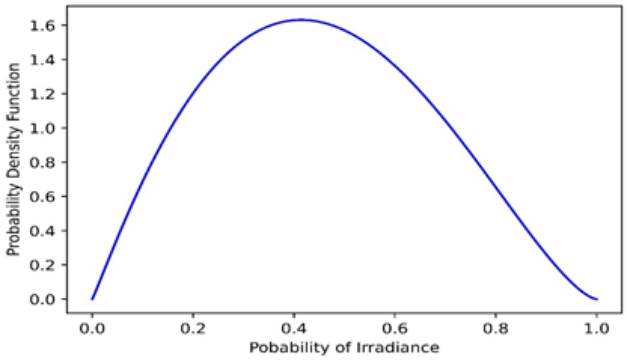

Figure 4: PDF of solar irradiance level using beta distribution

3.1.3 Load Model

Figure 5 presents the probability density function of the load model. The figure indicates the maximum chance of occurrence of load around the mean of the loads of the IEEE-9 bus system with the normal distribution. The probability of the load ranges from 50MW to 150MW, with a higher value of the probability of occurrence.

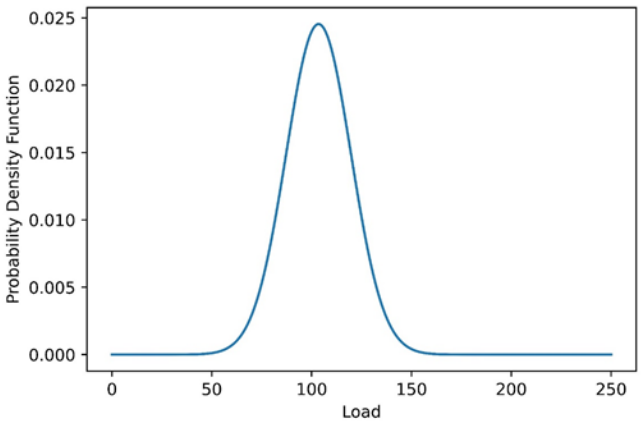

Figure 5: PDF of load for IEEE-9 bus system

3.1.4 Load Flow Analysis

The load flow was performed using the power flow equations and the voltage profile of the system is depicted in Figure 6. The loss on each of the branches is shown in Figure 7. Line 3 (Bus5 - Bus7) is the most loss-occurring part of the system. Overall, the system suffers an active power loss of 1.46%.

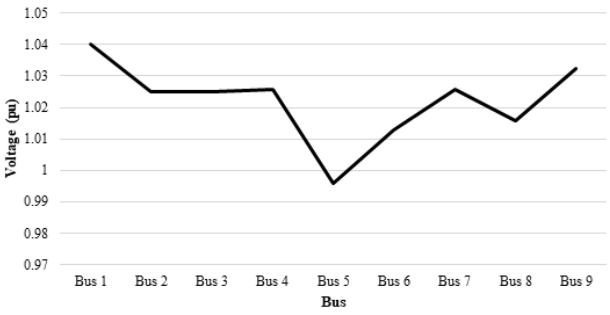

Figure 6: Bus voltages for IEEE-9 bus system

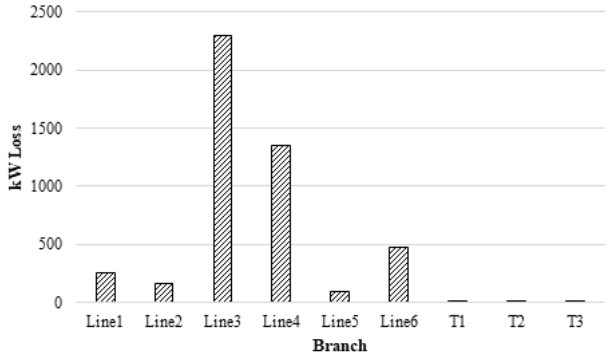

Figure 7: Loss in the branches of IEEE-9 bus system

3.1.5 Load Margin

Figure 8 illustrates the probability density function of the load margin with the correlated variables. The graph indicates that the probability of the system is most stable with the load increment by 20%. As the load increases beyond the factor of 1.3, there is less chance for the system to be stable.

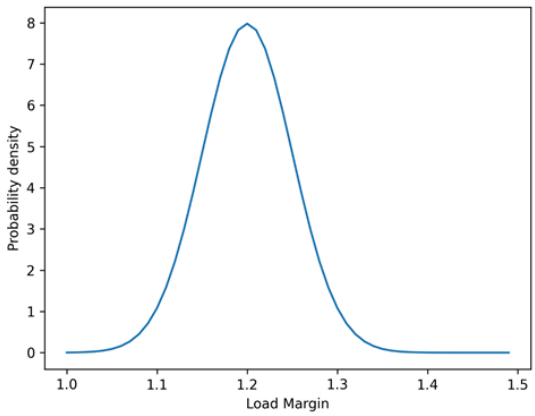

Figure 8: PDF of load margin

3.1.6 Sensitivity Analysis

The sensitivity indices of the different variations of load on the IEEE-9 bus system are compared in Table 1. The sensitivity of the active load on bus 8 is the highest followed by that on bus 5 and then bus 6. The reactive power of the loads has a lower significance on the overall stability of the system.

Table 1: Ranking of the load parameters of IEEE-9 bus

Variable	Sensitivity	Ranking
Active Power on Bus 5	0.221	2
Active Power on Bus 6	0.188	3
Active Power on Bus 8	0.529	1
Reactive Power on Bus 5	0.009	5
Reactive Power on Bus 6	0.005	6
Reactive Power on Bus 8	0.03	4

Figure 9 presents the probability density function of the load margin for different cases considering various loads constant. The system has the highest probability of being stable with active power on bus-8 constant.

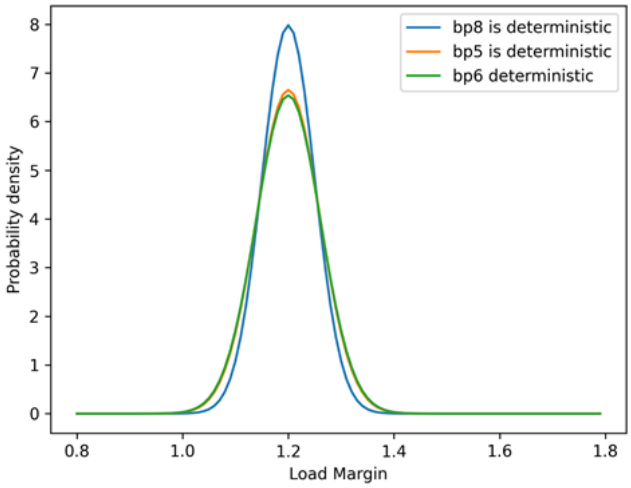

Figure 9: PDF at various cases of load in IEEE-9 bus

3.1.7 PV-QV curves

Figure 10 represents the P-V curve for the load buses on buses 5, 6, and 8 considered. The figure shows that on increasing the load on the specific bus, the system will become unstable if the load is increased by around 450MW.

Figure 11 represents the Q-V curve for the load on the load buses considered. The figure represents that on increasing the load on the specific bus, the system will become unstable if the reactive load is increased by around 275MVar.

3.2 INPS of Lumbini Province

The results obtained from the analysis of INPS of Lumbini Province is described in this section.

3.2.1 Evaluation of Wind Parameters

The study in Lumbini province evaluates wind generation, analyzing recorded wind velocities to determine 'k' and 'c' parameters using the Weibull distribution model. Figure 12

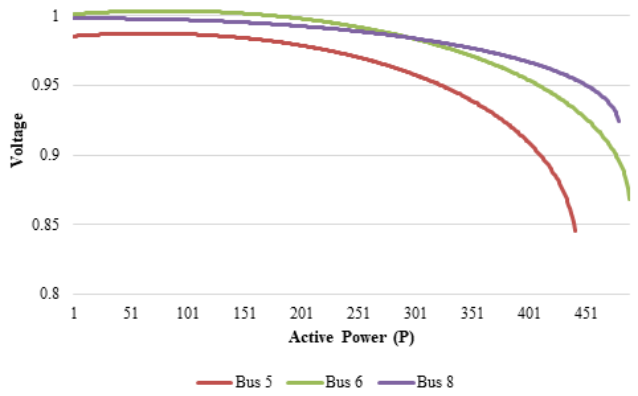

Figure 10: PV curve with active power variations in Load bus

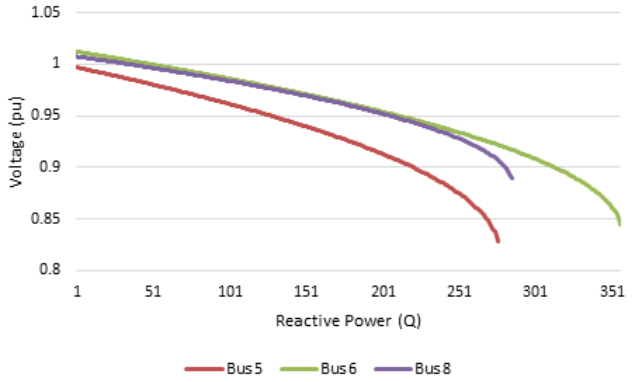

Figure 11: QV curve with reactive power variations in Load bus

presents detailed analyses of Purungchheda, Dang, Koilabas, and Sitapur, showcasing 'k' values indicating wind generation consistency. Purungchheda, Dang, maintains 'k' values from 2.02 to 2.24, suggesting reliability with moderate variability. Koilabas exhibits consistent patterns with 'k' values between 2.15 and 2.27. Sitapur's fluctuating 'k' values (1.99 to 2.26) imply broader distribution and higher variability. 'c' values signify energy potential, with Purungchheda, Dang, indicating higher wind speeds (5.47 to 5.93). Koilabas and Sitapur exhibit moderate to high energy generation potential.

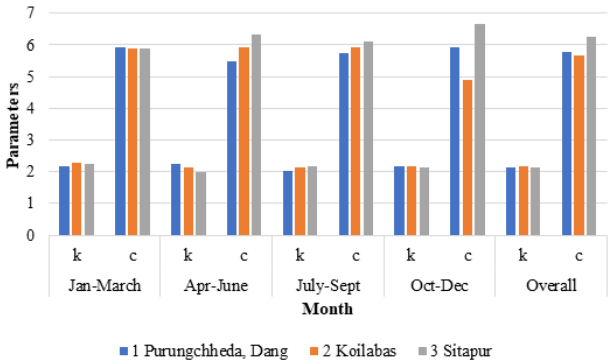

Figure 12: Seasonal k and c values for wind generation locations

3.2.2 Evaluation of PV Parameters

The study determines stochastic variables for PV and wind generations, analyzing parameters season-wise and overall. Figure 13 illustrates these parameters for solar projects, categorized by seasons and an 'Overall' column consolidating 'a' and 'b' values, providing insights into the distinctive characteristics of solar power generation. The interplay between 'alpha' and 'beta' values reveals stability, reliability, and predictability, aiding energy planners in understanding challenges and opportunities associated with each solar installation. Variations in 'a' and 'b' parameters across seasons indicate seasonal dynamics, with higher 'a' values suggesting stable generation and lower 'a' values indicating greater variability.

3.2.3 Load Flow Analysis

The load flow analysis of Lumbini province's electrical system reveals varying voltage levels at substations, as indicated in Figure 14, ranging from 0.817 to 0.99 pu. Jhumruk PH and Chandrauti Grid SS show the highest levels (0.99 and 0.976 pu), indicating well-regulated and stable voltage supply, while lower levels at Bastu SS, Lumbini SS, and Parasi SS (0.817, 0.826, and 0.8265 pu) suggest potential needs for voltage regulation measures.

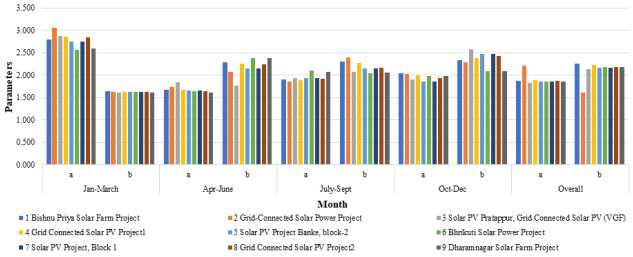

Figure 13: Seasonal a and b values for PV generation locations

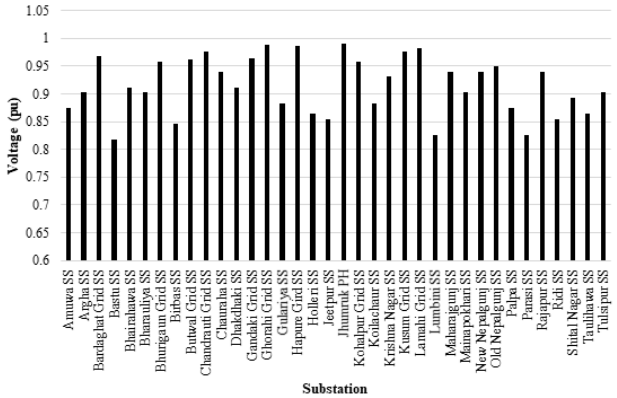

Figure 14: Voltages of substation in Lumbini Province

Similarly, the line loss is dominant in the line from the Butwal grid substation to the Dhakdahi substation with a power loss of 10.44%. Similarly, the 33kV line from Old Nepalgunj to Nanpara suffers a loss of 8.97% while the line from Chandrauta – Jeetpur Tapping suffers 8.07% of the total sending power.

3.2.4 Correlation Matrix and Load Margins

Most solar projects exhibit strong positive correlations ranging from 0.8 to 1, indicating a close relationship between their power generation outputs. For example, "Bishnu Priya Solar Farm Project" shows strong positive correlations with almost all other solar projects, suggesting shared influences from similar weather conditions or geographical factors. Conversely, correlations between wind generation locations ("Purungchheda, Dang," "Koilabas," and "Sitapur") and solar projects are generally low, ranging from -0.01 to 0.19, implying that wind and solar generation in these locations operate somewhat independently.

Figure 15 illustrates the impact of renewable energy sources (RES) on overall system stability in Lumbini province, with "Uncorrelated" and "Correlated" indicating the degree of independence among RES. The load margin values, ranging from 0.94 to 1.53, consistently exceed 1, reflecting a reliable and stable power supply in the region, with variations in the proportions of renewable energy sources over time. Despite slight differences in energy generation, both Uncorrelated and Correlated RES contribute to a consistently stable power supply, as reflected in load margin values consistently above 1.

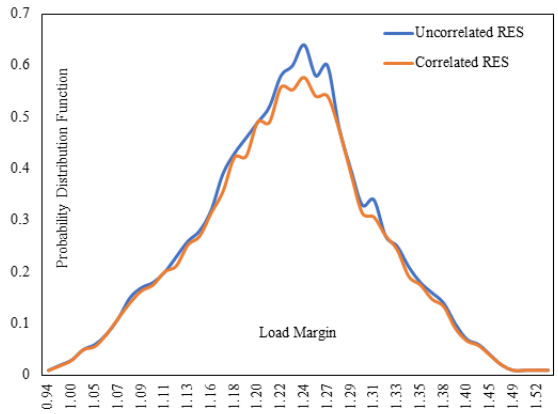

Figure 15: PDF of load margin for the system of Lumbini province for correlated and uncorrelated generation

3.2.5 Sensitivity Indices

Table 2 displays sensitivity indices and rankings for active power variation of major five substations, highlighting "Butwal Grid SS" as the most influential with a high sensitivity index of 0.3684, indicating its critical role in overall active power management. "Bhairahawa SS" follows with a sensitivity index of 0.0785, emphasizing its importance, while "Parasi SS" ranks third with a sensitivity index of 0.0631, indicating its significant role in maintaining stable active power levels. In contrast, substations like "Hapure Gird SS," "Kusum Grid SS," and "Taulihawa SS" have lower sensitivity indices, suggesting a relatively minor impact on active power variations within the province.

Figure 16 presents Probability Density Function (PDF) graphs for load margin values under deterministic scenarios (Butwal Grid, Bhairahawa SS, and Parasi SS). The Butwal Grid scenario exhibits a gradual increase in PDF with a peak around 1.28, suggesting higher stability, while Bhairahawa SS shows a pronounced peak around 1.27 with higher variability. Parasi SS has a peak around 1.2 with a skewed distribution toward higher load margin values. These variations indicate differences in load margin probability distributions, highlighting Butwal Grid's sensitivity and contribution to overall system stability. The trend is followed by Bhairahawa and Parasi substation scenarios in the same order of sensitivity.

Table 2: Ranking of the load parameters of INPS at Lumbini Province

Substation	Sensitivity Index	Ranking
Butwal Grid	0.3684	1
Bhairahawa	0.0785	2
Parasi	0.0631	3
Bardaghat Grid	0.0412	4
Jeetpur	0.03	5

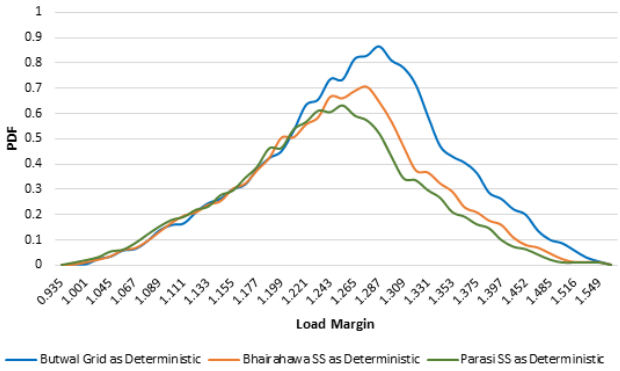

Figure 16: PDF of load margin for the system of Lumbini province for correlated and uncorrelated generation

3.2.6 PV-QV Curves

Figure 17 depicts the Active Power-Voltage curve, revealing the dynamic relationship between voltage levels and active power for Butwal, Bhairahawa, and Parasi substations; notably, Butwal consistently exhibits higher active power values across the voltage range, indicating a characteristic trend of voltage decrease with increasing active power, while Bhairahawa and Parasi, having smaller conductors, experience more significant voltage drop.

Figure 18 demonstrates the Reactive Power-Voltage curves for Butwal, Bhairahawa, and Parasi substations, with Butwal displaying a broader range of reactive power increment due to higher transmission line capacity, resulting in a more significant voltage drop compared to Bhairahawa and Parasi substations and some improvement in voltage profile and power carrying capacity with the RES.

4. Conclusion

The results unveiled a 1.46% power loss with minimum voltage at Bus 5, and load margin analysis identified a probable value around 1.2 times the existing load for IEEE-9 bus system. In case of INPS of Lumbini Province, Sensitivity analysis pinpointed Butwal Grid SS as the most influential substation for active power variation, underscoring its critical

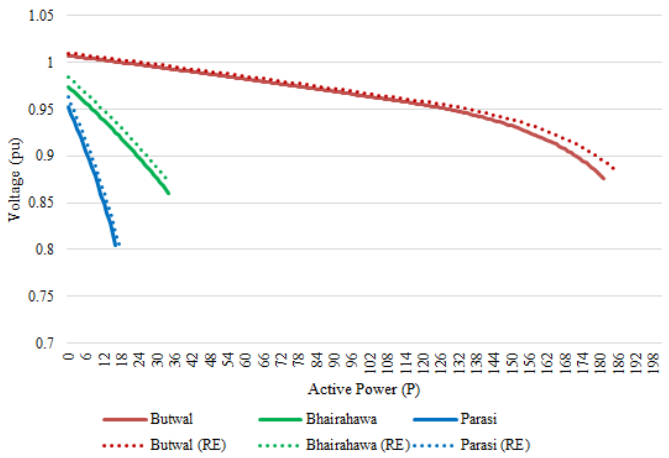

Figure 17: P-V curve for the variation of load in the major substations

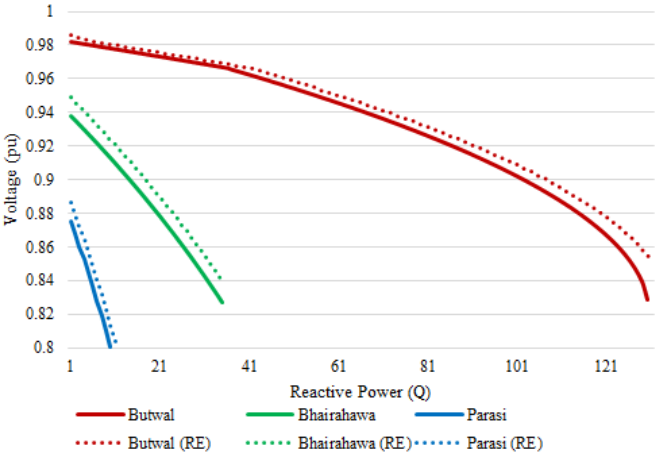

Figure 18: Q-V curve for the variation of load in the major substations

role in power distribution. Wind generation analysis in Lumbini province revealed distinctive patterns across locations, emphasizing the uniqueness of each area's wind characteristics. Correlation analysis indicated strong positive correlations among solar projects, while load margin values consistently exceeding 1 highlighted the reliability of Lumbini Province's power supply. The study offers a foundation for future research on time-dependent generation variations and expanding optimal power flow analysis to larger and more complex power systems.

Acknowledgments

The authors are thankful to Energize Nepal (ENEP) for funding this research work and to the faculty members of Department of Electrical Engineering, Pashchimanchal Campus, TU for their support.

References

[1] Wujing Huang, Ning Zhang, Jingwei Yang, Yi Wang, and Chongqing Kang. Optimal configuration planning of multi-energy systems considering distributed renewable energy. *IEEE Transactions on Smart Grid*, 10(2):1452–1464, 2019.

[2] C.O. Nwankpa, S.M. Shahidehpour, and Z. Schuss. A stochastic approach to small disturbance stability analysis. *IEEE Transactions on Power Systems*, 7(4):1519–1528, 1992.

[3] Barbara Borkowska. Probabilistic load flow. *IEEE Transactions on Power Apparatus and Systems*, PAS-93(3):752–759, 1974.

[4] S. Q. Bu, W. Du, H. F. Wang, Z. Chen, L. Y. Xiao, and H. F. Li. Probabilistic analysis of small-signal stability of large-scale power systems as affected by penetration of wind generation. *IEEE Transactions on Power Systems*, 27(2):762–770, 2012.

[5] Wah Cheung Wong, C. Y. Chung, Ka Wing Chan, and Haoyong Chen. Quasi-monte carlo based probabilistic small signal stability analysis for power systems with plug-in electric vehicle and wind power integration. *IEEE Transactions on Power Systems*, 28(3):3335–3343, 2013.

[6] Fei Ni, Phuong H. Nguyen, and Joseph F. G. Cobben. Basis-adaptive sparse polynomial chaos expansion for probabilistic power flow. *IEEE Transactions on Power Systems*, 32(1):694–704, 2017.

[7] Xiaoyuan Xu and Zheng Yan. Probabilistic load flow calculation with quasi-monte carlo and multiple linear regression. *International Journal of Electrical Power & Energy Systems*, 88:1–12, 2017.

[8] S. Greene, I. Dobson, and F.L. Alvarado. Sensitivity of the loading margin to voltage collapse with respect to arbitrary parameters. *IEEE Transactions on Power Systems*, 12(1):262–272, 1997.

[9] N. Amjady and M. Esmaili. Application of a new sensitivity analysis framework for voltage contingency ranking. *IEEE Transactions on Power Systems*, 20(2):973–983, 2005.

[10] Xiaoyuan Xu, Zheng Yan, Mohammad Shahidehpour, Han Wang, and Sijie Chen. Power system voltage stability evaluation considering renewable energy with correlated variabilities. *IEEE Transactions on Power Systems*, 33(3):3236–3245, 2018.

[11] R. Ian Harris and Nicholas J. Cook. The parent wind speed distribution: Why weibull? *Journal of Wind Engineering and Industrial Aerodynamics*, 131:72–87, 2014.